Inorg. Chem. **2005**, *44*, 8379–8390

Synthesis of the Five-Coordinate Ruthenium(II) Complexes [(PCP)Ru(CO)(L)][BAr′$_4$] {PCP = 2,6-(CH$_2$P^{t}Bu$_2$)$_2$C$_6$H$_3$, BAr′$_4$ = 3,5-(CF$_3$)$_2$C$_6$H$_3$, L = η^1-ClCH$_2$Cl, η^1-N$_2$, or μ-Cl–Ru(PCP)(CO)}: Reactions with Phenyldiazomethane and Phenylacetylene

Jubo Zhang,[†] Khaldoon A. Barakat,[‡] Thomas R. Cundari,[‡] T. Brent Gunnoe,*[,†] Paul D. Boyle,[†] Jeffrey L. Petersen,[§] and Cynthia S. Day[||]

Department of Chemistry, North Carolina State University, Raleigh, North Carolina 27695-8204, Department of Chemistry, University of North Texas, Box 305070, Denton, Texas 76203-5070, C. Eugene Bennett Department of Chemistry, West Virginia University, Morgantown, West Virginia 26506-6045, and Department of Chemistry, Wake Forest University, Winston Salem, North Carolina 27109-7486

Received June 29, 2005

Reaction of (PCP)Ru(CO)(Cl) (**1**) with NaBAr′$_4$ yields the bimetallic product [{(PCP)Ru(CO)}$_2$(μ-Cl)][BAr′$_4$] (**2**). The monomeric five-coordinate complexes [(PCP)Ru(CO)(η^1-ClCH$_2$Cl)][BAr′$_4$] (**3**) and [(PCP)Ru(CO)(η^1-N$_2$)][BAr′$_4$] (**4**) are synthesized upon reaction of (PCP)Ru(CO)(OTf) (**6**) with NaBAr′$_4$ in CH$_2$Cl$_2$ or C$_6$H$_5$F, respectively. The solid-state structures of **2**, **3**, and **4** have been determined by X-ray diffraction studies of single crystals. The reaction of **3** with PhCHN$_2$ or PhC≡CH affords carbon–carbon coupling products involving the aryl group of the PCP ligand in transformations that likely proceed via the formation of Ru carbene or vinylidene intermediates. Density functional theory and hybrid quantum mechanics/molecular mechanics calculations were performed to investigate the bonding of weak bases to the 14-electron fragment [(PCP)Ru(CO)]$^+$ and the energetics of different isomers of the product carbene and vinylidene complexes.

Introduction

Coordinatively and electronically unsaturated divalent ruthenium complexes with 14- or 16-electron counts are of interest as possible intermediates in catalytic processes as well as for the fundamental understanding of structure and bonding.[1,2] For example, 16-electron Grubbs-type ruthenium catalysts have been successfully applied to olefin metathesis,[3−5] coordinatively unsaturated half-sandwich ruthenium complexes with phosphine, amidinate, or carbene ligands have been extensively studied,[6−13] and several unsaturated ruthenium complexes have been synthesized to study C−H agostic interactions.[14−17] Caulton et al. have conducted systematic studies on the synthesis and reactivity of four-coordinate

* To whom correspondence should be addressed. E-mail: brent_gunnoe@ncsu.edu.
[†] North Carolina State University.
[‡] University of North Texas.
[§] West Virginia University.
[||] Wake Forest University.

(1) Collman, J. P.; Hegedus, L. S.; Norton, J. R.; Finke, R. G. *Principles and Applications of Organotransition Metal Chemistry*; University Science: Mill Valley, CA, 1987.
(2) Crabtree, R. H. *The Organometallic Chemistry of the Transition Metals*, 2nd ed.; John Wiley and Sons: New York, 1994.
(3) Trnka, T. M.; Grubbs, R. H. *Acc. Chem. Res.* **2001**, *34*, 18−29.
(4) Grubbs, R. H.; Chang, S. *Tetrahedron* **1998**, *54*, 4413−4450.
(5) Grubbs, R. H. *Tetrahedron* **2004**, *60*, 7117−7140.
(6) Nagashima, H.; Kondo, H.; Hayashida, T.; Yamaguchi, Y.; Gondo, M.; Masuda, S.; Miyazaki, K.; Matsubara, K.; Kirchner, K. *Coord. Chem. Rev.* **2003**, *245*, 177−190.
(7) Aneetha, H.; Jiménez-Tenorio, M.; Puerta, M. C.; Valerga, P.; Sapunov, V. N.; Schmid, R.; Kirchner, K.; Mereiter, K. *Organometallics* **2002**, *21*, 5334−5346.
(8) Tenorio, M. J.; Puerta, M. C.; Valerga, P. *J. Organomet. Chem.* **2000**, *609*, 161−168.
(9) Kolle, U.; Rietmann, C.; Raabe, G. *Organometallics* **1997**, *16*, 3273−3281.
(10) Campion, B. K.; Heyn, R. H.; Tilley, T. D. *J. Chem. Soc., Chem. Commun.* **1988**, 278.
(11) Johnson, T. J.; Huffman, J. C.; Caulton, K. G. *J. Am. Chem. Soc.* **1992**, *114*, 2725−2726.
(12) Bickford, C. C.; Johnson, T. J.; Davidson, E. R.; Caulton, K. G. *Inorg. Chem.* **1994**, *33*, 1080.
(13) Huang, J.; Stevens, E. D.; Nolan, S. P.; Petersen, J. L. *J. Am. Chem. Soc.* **1999**, *121*, 2674−2678.
(14) Huang, D.; Streib, W. E.; Eisenstein, O.; Caulton, K. G. *Angew. Chem., Int. Ed. Engl.* **1997**, *36*, 2004−2006.
(15) Tenorio, M. J.; Tenorio, M. A. J.; Puerta, M. C.; Valerga, P. *Inorg. Chim. Acta* **1997**, *259*, 77−84.

10.1021/ic051074k CCC: $30.25
Published on Web 10/06/2005

complexes of the type $[L_2Ru(CO)(R)][BAr'_4]$ (R = H, Me, or Ph; Ar′ = 3,5-$(CF_3)_2C_6H_3$; L = phosphine ligands) as well as their five-coordinate precursors and have extended their studies to systems with the chelating PNP (PNP = $N(SiMe_2CH_2PR_2)_2$, R = Cy or ^{t}Bu) ligands.[14,18−23]

Our group has been interested in studying the reactivity of coordinatively unsaturated ruthenium complexes with a bulky PCP pincer ligand (PCP = 2,6-$(CH_2P^tBu_2)_2C_6H_3$), and we have previously reported the synthesis of the amido complexes (PCP)Ru(CO)(NHR) (R = H or Ph) and their reactivity with substrates that possess polar as well as nonpolar bonds.[24−26] For example, the ruthenium parent amido complex (PCP)Ru(CO)(NH_2) has been demonstrated to initiate the activation of dihydrogen as well as the intramolecular activation of C−H bonds.[24] The reaction of (PCP)Ru(CO)(PMe_3)(NHPh) with organic substrates such as nitriles, carbodiimides, and isocyanates likely proceeds via PMe_3 dissociation, coordination of the organic substrate, and intramolecular nucleophilic addition of the amido nitrogen to form azametallacyclobutane complexes.[25,26] Herein, we report that efforts to access a four-coordinate ruthenium complex starting from the five-coordinate precursor (PCP)Ru(CO)(Cl) (**1**) lead to the formation of complexes of the type $[(PCP)Ru(CO)(L)]^+$ {L = η^1-$ClCH_2Cl$, η^1-N_2, C_6H_5F, or μ-Cl−Ru(PCP)(CO)}.[27] We anticipated that the geometrical restriction of the meridional coordinating tridentate PCP ligand might lead to chemistry that diverges from that of Caulton et al.'s $[L_2Ru(CO)(R)]^+$ systems. Reactions of $[(PCP)Ru(CO)(ClCH_2Cl)]^+$ with a carbene source or a phenylacetylene yield products that are intermediates for carbene or vinylidene insertion into the Ru aryl bond of the PCP ligand. Computational studies of these systems are also presented and discussed.

Results and Discussions

Synthesis and Solid-State Structures of [{(PCP)Ru(CO)}$_2$(μ-Cl)][BAr′$_4$] (2), [(PCP)Ru(CO)(η^1-$ClCH_2Cl$)][BAr′$_4$] (3), and [(PCP)Ru(CO)(η^1-N_2)][BAr′$_4$] (4). The air stable 16-electron compound **1** has been synthesized and structurally characterized by Gusev and co-workers.[27] Chloride abstraction from **1** could afford a four-coordinate ruthenium center; however, the reaction of complex **1** with 1 equiv of $NaBAr'_4$ in CH_2Cl_2 results in the formation of a mixture of two products that could not be separated. Given the possibility of formation of a binuclear species with a bridging chloride ligand, we reacted complex **1** with 0.5 equiv of $NaBAr'_4$. Clean isolation of the complex [{(PCP)Ru(CO)}$_2$(μ-Cl)][BAr′$_4$] (**2**) in 80% yield was obtained after workup (eq 1). Complex **2** is air sensitive, as indicated by

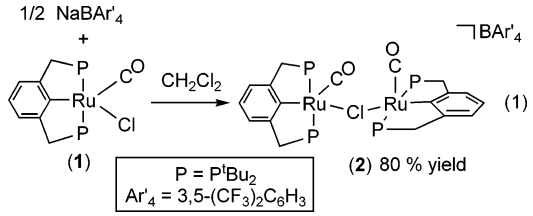

slow decomposition of a CD_2Cl_2 solution of **2** in air. Salient features of the ^{1}H NMR spectrum of **2** include overlapping multiplets in the region 1.74−0.85 ppm due to the PCP *tert*-butyl groups, as compared to two virtual triplets for **1**.[27] Also, doublets at 74.1 and 68.9 ppm (J_{PP} = 228 Hz) are observed in the ^{31}P NMR spectrum of **2**, while IR spectroscopy reveals ν_{CO} = 1939 cm^{-1}. Further reaction of **2** with $NaBAr'_4$ or reaction of **1** with excess $NaBAr'_4$ results in a mixture of complex **2** and a second product; however, the second product could not be isolated cleanly.

A single crystal of **2** grown from a methylene chloride solution layered with pentane was selected for an X-ray diffraction study. A limited resolution data set revealed the presence of two {(PCP)Ru(CO)} fragments connected with a bridging chloride (Figure 1). The low yield of high-resolution data for this compound is presumably due to the presence of disordered CH_2Cl_2 and pentane solvent molecules of crystallization as well as disordered CF_3 groups of the anion. Nonetheless, the X-ray data are consistent with the assigned structure based on spectroscopic and elemental analysis data.

As reported previously, the treatment of complex **1** with excess trimethylsilyltriflate (TMSOTf) affords (PCP)Ru(CO)(OTf) (OTf = η^1-OSO_2CF_3) (**6**).[25] When 1 equiv of $NaBAr'_4$ was added to a CH_2Cl_2 solution of **6**, the CO

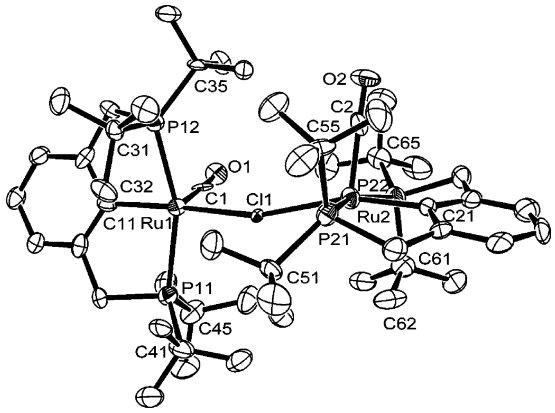

Figure 1. ORTEP diagram (30% probability) of [{(PCP)Ru(CO)}$_2$(μ-Cl)][BAr′$_4$] (**2**) (hydrogen atoms and the BAr'_4 counterion have been omitted for clarity).

(16) Baratta, W.; Herdtweck, E.; Rigo, P. *Angew. Chem., Int. Ed.* **1999**, *38*, 1629−1631.
(17) Tenorio, M. J.; Mereiter, K.; Puerta, M. C.; Valerga, P. *J. Am. Chem. Soc.* **2000**, *122*, 11230−11231.
(18) Huang, D.; Streib, W. E.; Bollinger, J. C.; Caulton, K. G.; Winter, R. F.; Scheiring, T. *J. Am. Chem. Soc.* **1999**, *121*, 8087−8097.
(19) Huang, D.; Bollinger, J. C.; Streib, W. E.; Folting, K.; Young, V., Jr.; Eisenstein, O.; Caulton, K. G. *Organometallics* **2000**, *19*, 2281−2290.
(20) Watson, L. A.; Coalter, J. N., III; Ozerov, O. V.; Pink, M.; Huffman, J. C.; Caulton, K. G. *New J. Chem.* **2003**, 263.
(21) Watson, L. A.; Ozerov, O. V.; Pink, M.; Caulton, K. G. *J. Am. Chem. Soc.* **2003**, *125*, 8426−8427.
(22) Walstrom, A. N.; Watson, L. A.; Pink, M.; Caulton, K. G. *Organometallics* **2004**, *23*, 4814−4816.
(23) Walstrom, A.; Pink, M.; Yang, X.; Tomaszewski, J.; Baik, M.-H.; Caulton, K. G. *J. Am. Chem. Soc.* **2005**, *127*, 5330−5331.
(24) Conner, D.; Jayaprakash, K. N.; Cundari, T. R.; Gunnoe, T. B. *Organometallics* **2004**, *23*, 2724−2733.
(25) Zhang, J.; Gunnoe, T. B.; Boyle, P. D. *Organometallics* **2004**, *23*, 3094−3097.
(26) Zhang, J.; Gunnoe, T. B.; Petersen, J. L. *Inorg. Chem.* **2005**, *44*, 2895−2907.
(27) Gusev, D. G.; Madott, M.; Dolgushin, F. M.; Lyssenko, K. A.; Antipin, M. Y. *Organometallics* **2000**, *19*, 1734−1739.

Scheme 1. Reaction of (PCP)Ru(CO)(OTf) (**6**) with $NaBAr'_4$ in CH_2Cl_2 or in C_6H_5F[a]

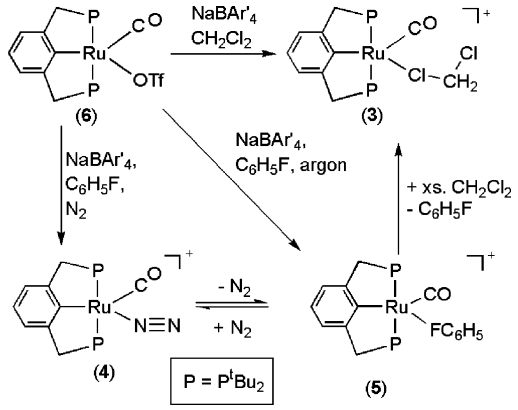

[a] Complex **5** has not been fully characterized, and its identity is suggested based on evidence from IR spectroscopy and computational studies.

absorption changed from 1941 to 1964 cm^{-1} within 30 min, as determined by IR spectroscopy. A highly air sensitive product that turns black immediately upon exposure to air can be isolated after workup. Characterization using ^1H, ^{31}P, and ^{19}F NMR and IR spectroscopy as well as X-ray crystallography revealed the complex as [(PCP)Ru(CO)(η^1-$ClCH_2Cl$)][BAr'_4] (**3**) (Scheme 1).

Instead of formation of a four-coordinate complex, a molecule of CH_2Cl_2 coordinates to the ruthenium center through a single chlorine atom. A singlet at 5.35 ppm in the ^1H NMR spectrum of **3** in CD_2Cl_2 is most likely due to free CH_2Cl_2 as a result of rapid exchange of coordinated CH_2Cl_2 with CD_2Cl_2. The PCP ligand yields two virtual triplets at 1.50 and 1.11 ppm (N = 15 Hz) in the ^1H NMR spectrum and a broad singlet at 71.0 ppm in the ^{31}P NMR spectrum of **3**.

Although the fragment $[(PCP)Ru(CO)]^+$ has two available coordination sites, the X-ray structural analysis of **3** confirmed the presence of a monohapto coordinated η^1-CH_2Cl_2 ligand (Figure 2). The bond length of Ru1−Cl1s (2.614(1) Å) is longer than the Ru−Cl bond distance in **1** (2.420(1) Å). The C−Cl (bound) distance is 1.791(5) Å while the C−Cl (unbound) distance is 1.695(5) Å. The Cl−C−Cl bond angle is 115.5(2)° with the unbound Cl oriented toward the carbonyl group. One agostic interaction is indicated based on the short $Ru/C_{agostic}$ distance (Ru1···C23, 2.85(1) Å), and the bond angle Ru1−P2−C22 (100.9(1)°) is significantly smaller than the other three *tert*-butyl group bond angles (113.4(1)°, 121.8(1)°, and 127.8(1)°). Previously, Caulton et al. observed double agostic interactions for the complex [Ru(Ph)(CO)(P^tBu_2Me)$_2$][BAr'_4] with $Ru/C_{agostic}$ bond lengths of 2.87 and 2.88 Å and Ru−P−C bond angles of 98.1° and 96.6°.[14] An agostic interaction has been observed in the solid-state structure of $[(PCP)Ru(CO)_2]^+$ with a reported Ru···HC distance of 2.19(6) Å.[28] Although both bidentate and monodentate CH_2Cl_2 ligands have been reported, examples of structurally characterized complexes with CH_2Cl_2 ligands are relatively rare.[19,29−36] For example, the synthesis and solid-state structures of [$RuH(CO)(PMe^tBu_2)_2(\eta^2$-$CH_2Cl_2)$][$BAr'_4$], [$Cp^*Ir(Me)(\eta^1$-$ClCH_2Cl)$][$BAr'_4$], [*trans*-$(P^iPr_3)_2Pt(H)(\eta^1$-$ClCH_2Cl)$][$BAr'_4$], and [*cis*-$Re(CO)_4(PPh_3)(\eta^1$-$ClCH_2Cl)$]-[$BAr'_4$] have been reported ($Cp^*$ = pentamethylcyclopentadienyl).[19,30−32] The ruthenium hydride complex [$Ru(H)(\eta^2$-$CH_2Cl_2)(CO)(P^tBu_2Me)_2$][$BAr'_4$] with an η^2-coordinated CH_2Cl_2 has been reported, while the closely related ruthenium phenyl compound [Ru(Ph)(CO)(P^tBu_2Me)][BAr'_4] could be crystallized from a CH_2Cl_2 solution without evidence of CH_2Cl_2 coordination.[14,19] Complexes with other chloroalkanes or chlorobenzene ligands have been reported.[33,37−39]

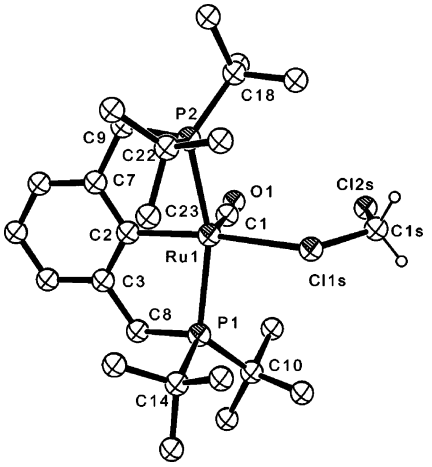

Figure 2. ORTEP diagram (30% probability) of [(PCP)Ru(CO)(η^1-$ClCH_2Cl$)][BAr'_4] (**3**) (hydrogen atoms, except the two on CH_2Cl_2, and the BAr'_4 counterion have been omitted for clarity). Selected bond lengths (Å) and bond angles (deg): Ru1−Cl1s, 2.614(1); Ru1−C2, 2.053(3); C1s−Cl1s, 1.791(5); C1s−Cl2s, 1.695(5); Cl1s−C1s−Cl2s, 115.5(2); Ru1−Cl1s−C1s, 123.1(2); C2−Ru1−Cl1s, 170.7(2); Ru1−P2−C22, 100.9(1); Ru1−P2−C18, 127.8(1); Ru1−P1−C14, 113.4(1); Ru1−P1−C10, 121.8(1); P1−Ru1−P2, 161.5(1).

To exclude the possibility of CH_2Cl_2 coordination, 1 equiv of $NaBAr'_4$ was reacted with **6** in fluorobenzene. IR spectroscopy revealed two CO absorptions at 1987 cm^{-1} (major) and 1953 cm^{-1} (minor). In addition, an absorption at 2249 cm^{-1} was observed and assigned to coordinated dinitrogen. Free dinitrogen exhibits an absorption at 2331 cm^{-1} (Raman).[1,2] Purging the solution with argon results in the transformation to a solution with a single CO absorption at 1953 cm^{-1} and the disappearance of absorptions previously

(28) van der Boom, M. E.; Iron, M. A.; Atasoylu, O.; Shimon, L. J. W.; Rozenberg, H.; Ben-David, Y.; Konstantinovski, L.; Martin, J. M. L.; Milstein, D. *Inorg. Chim. Acta* **2004**, *357*, 1854−1864.

(29) Kulawiec, R. J.; Crabtree, R. H. *Coord. Chem. Rev.* **1990**, *99*, 89.
(30) Arndtsen, B. A.; Bergman, R. G. *Science* **1995**, *270*, 1970−1972.
(31) Butts, M. D.; Scott, B. L.; Kubas, G. J. *J. Am. Chem. Soc.* **1996**, *118*, 11831−11843.
(32) Huhmann-Vincent, J.; Scott, B. L.; Kubas, G. J. *J. Am. Chem. Soc.* **1998**, *120*, 6808−6809.
(33) Peng, T.-S.; Winter, C. H.; Gladysz, J. A. *Inorg. Chem.* **1994**, *33*, 2534−2542.
(34) Colsman, M. R.; Newbound, T. D.; Marshall, L. J.; Noirot, M. D.; Miller, M. M.; Wulfsberg, G. P.; Frye, J. S.; Anderson, O. P.; Strauss, S. H. *J. Am. Chem. Soc.* **1990**, *112*, 2349−2362.
(35) Newbound, T. D.; Colsman, M. R.; Miller, M. M.; Wulfsberg, G. P.; Anderson, O. P.; Strauss, S. H. *J. Am. Chem. Soc.* **1989**, *111*, 3762−3764.
(36) Bown, M.; Waters, J. M. *J. Am. Chem. Soc.* **1990**, *112*, 2442−2443.
(37) Van Seggen, D. M.; Anderson, O. P.; Strauss, S. H. *Inorg. Chem.* **1992**, *31*, 2987−2990.
(38) Wu, F.; Dash, A. K.; Jordan, R. F. *J. Am. Chem. Soc.* **2004**, *126*, 15360−15361.
(39) Ben-Ari, E.; Gandelman, M.; Rozenberg, H.; Shimon, L. J. W.; Milstein, D. *J. Am. Chem. Soc.* **2003**, *125*, 4714−4715.

observed at 1987 and 2249 cm^{-1}. However, this change is reversible, as purging the resultant solution with dinitrogen leads to observation of the three original absorptions at 1987, 1953, and 2249 cm^{-1}. These results suggest an equilibrium between a five-coordinate dinitrogen complex, [(PCP)Ru(CO)(N_2)][BAr'_4] (**4**), with a labile N_2 ligand, and a second complex that is likely either the four-coordinate complex [(PCP)Ru(CO)][BAr'_4] or the fluorobenzene complex [(PCP)Ru(CO)(FC_6H_5)][BAr'_4]. Repeated attempts to grow crystals and perform an X-ray diffraction study of this complex have failed; however, on the basis of IR evidence, we propose that the coordination of fluorobenzene is more likely, though not definitively shown, than the formation of a four-coordinate system. For example, the series of Ru(II) systems Ru(Ph)(CO)(Cl)L_2, Ru(Ph)(CO)(OTf)L_2, and [Ru(Ph)(CO)L_2][BAr'_4] (where L = P^tBu_2Me and the latter complex is a four-coordinate system with two agostic interactions) exhibits CO absorptions (IR spectroscopy) at 1902, 1921, and 1958 cm^{-1}, respectively.[14,18,19] The series of systems (PCP)Ru(CO)(Cl), (PCP)Ru(CO)(OTf), and the uncharacterized complex has CO absorptions at 1919, 1941, and 1953 cm^{-1}. The conversion of the (PCP)Ru−Cl complex to the (PCP)Ru−OTf complex results in an increase in the CO stretching frequency of 22 cm^{-1}, while the conversion of the Ru(Ph)(CO)(Cl)L_2 complex to the corresponding triflate complex, Ru(Ph)(CO)(OTf)L_2, results in an increase in the CO stretching frequency of 19 cm^{-1}. Thus, for the two types of Ru systems, conversion of a Ru−Cl bond to a Ru−OTf bond yields quite similar changes in the energy of the CO stretches. The conversion of the five-coordinate complex Ru(Ph)(CO)(OTf)L_2 to the four-coordinate complex [Ru(CO)(Ph)L_2][BAr'_4] increases the CO absorption energy by 37 cm^{-1}, while the transformation of (PCP)Ru(CO)(OTf) to complex **5** results in an increase of the CO absorption energy of only 12 cm^{-1}. Thus, without confirmation by X-ray crystallography, we assign the identity of this system as [(PCP)Ru(CO)(FC_6H_5)][BAr'_4] (**5**) (Scheme 1), and calculations are consistent with the notion that the coordination of fluorobenzene is favorable to a four-coordinate complex (see below). The formation of a binuclear species with a bridging dinitrogen ligand is another possibility for complex **5**; however, the reaction of (PCP)Ru(CO)(OTf) with $NaBAr'_4$ in C_6H_5F under argon produces complex **5** (as indicated by IR spectroscopy) and provides evidence against a complex that possesses a bridging dinitrogen moiety. When an excess of CH_2Cl_2 is added to the solution of **4** and **5**, conversion to complex **3** is observed, as indicated by a single CO absorption at 1964 cm^{-1} in the IR spectrum (eq 2).

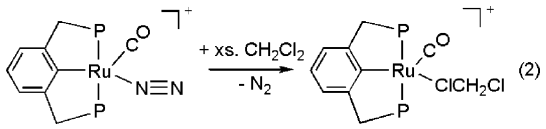

The identity of [(PCP)Ru(CO)(η^1-N_2)][BAr'_4] (**4**) has been confirmed by a single-crystal X-ray diffraction study (Figure 3). Similar to the case of complex **3**, one agostic interaction

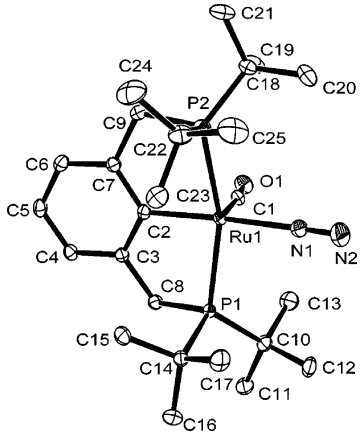

Figure 3. ORTEP diagram (30% probability) of [(PCP)Ru(CO)(η^1-N_2)][BAr'_4] (**4**) (hydrogen atoms and the BAr'_4 counterion have been omitted for clarity). Selected bond lengths (Å) and bond angles (deg): Ru1−C2, 2.059(2); Ru1−N1, 2.132(1); N1−N2, 1.069(3); Ru1−C1, 1.809(2); C1−O1, 1.148(2); N1−N2, 1.069(3); C2−Ru1−N1, 175.7(1); Ru1−N1−N2, 179.1(2); Ru1−P2−C22, 101.2(1); P1−Ru1−P2, 162.8(1).

is indicated by a short Ru/$C_{agostic}$ distance (Ru1···C23, 2.89 Å) and a small Ru−P−C bond angle (Ru1−P2−C22, 101.2(1)°). A Ru−N bond length of 2.132(1) Å and a linear Ru−N−N bond angle (179.1(2)°) are observed. The N1−N2 bond length (1.069(3) Å) is shorter than that in free N_2 (1.0975 Å);[40] however, correction of selected bond lengths for rigid body motion and riding effects resulted in a corrected N1−N2 bond length of 1.098 Å, which is indistinguishable from the N−N bond length in free dinitrogen (see the Supporting Information for details). A rhodium dinitrogen complex with an "aliphatic" PCP ligand, Rh(η^1-N_2){η^1-$CH_3C(CH_2CH_2P^tBu_2)_2$}, has been reported with a short N−N bond length of 0.963(14) Å.[41] Other complexes with short N−N bond lengths for dinitrogen ligands include *trans*-ReCl(N_2)(PMe_2Ph)$_2$ (1.055(30) Å), *trans*-RhCl(N_2)(P^iPr_3)$_2$ (0.958(5) Å), and *trans*-RhH(N_2)(PPh^tBu_2)$_2$ (1.074(7) Å) with the bond contraction due to disorder.[42−44] For complex **4**, the atom N2 displays a relatively high atomic displacement amplitude perpendicular to the N−N bond vector. However, there was no evidence of a multiple site orientational or compositional disorder in the final difference Fourier map (see the Supporting Information). The Ru−N bond distance of **4**, 2.132(1) Å, is longer than the bond distances of related Ru−dinitrogen complexes. For example, Ru(II) systems with bisphosphine "pincer" ligands with η^1-N_2 ligands have Ru−N bond distances in the range of 1.965(4)−2.014(2) Å.[45−47] For all of these systems, the observed dinitrogen stretching frequencies in

(40) Fryzuk, M. D.; Johnson, S. A. *Coord. Chem. Rev.* **2000**, *200*−*202*, 379−409.
(41) Vigalok, A.; Kraatz, H.-B.; Konstantinovski, L.; Milstein, D. *Chem.*−*Eur. J.* **1997**, *3*, 253−260.
(42) Ibers, J. A.; Mingos, D. M. P. *Inorg. Chem.* **1971**, *10*, 1035−1042.
(43) Hoffman, P. R.; Yoshida, T.; Okano, T.; Otsuka, S.; Ibers, J. A. *Inorg. Chem.* **1976**, *15*, 2462−2466.
(44) Thorn, D. L.; Tulip, T. H.; Ibers, J. A. *J. Chem. Soc., Dalton Trans.* **1979**, 2022−2025.
(45) Gusev, D. G.; Fontaine, F.-G.; Lough, A. J.; Zargarian, D. *Angew. Chem., Int. Ed.* **2003**, *42*, 216−219.
(46) Gusev, D. G.; Lough, A. J. *Organometallics* **2002**, *21*, 5091−5099.
(47) Amoroso, D.; Jabri, A.; Yap, G. P. A.; Gusev, D. G.; dos Santos, E. N.; Fogg, D. E. *Organometallics* **2004**, *23*, 4047−4054.

Table 1. Selected Crystallographic Data and Collection Parameters for Complexes **2**, **3**, **4**, **7**, and **8**

complex	[{(PCP)Ru(CO)}$_2$(μ-Cl)][BAr′$_4$] (**2**)	[(PCP)Ru(CO)(η^1-CH_2Cl_2)][BAr′$_4$] (**3**)	[(PCP)Ru(CO)(η^1-N_2)][BAr′$_4$] (**4**)	[(PCP−CHPh)Ru(CO)][BAr′$_4$] (**7**)	[(PCP−CCHPh)Ru(CO)][BAr′$_4$] (**8**)
empirical formula	$C_{93}H_{124}BCl_3F_{24}O_2P_4Ru_2$	$C_{58}H_{57}BCl_2F_{24}OP_2Ru$	$C_{66}H_{62.50}BF_{25.50}N_2OP_2Ru$	$C_{64}H_{61}BF_{24}P_2ORu$	$C_{66}H_{63}BCl_2F_{24}OP_2Ru$
formula wt	2173.10	1470.77	1558.01	1475.95	1572.88
cryst syst	monoclinic	triclinic	triclinic	triclinic	orthorhombic
space group	$P2_1/c$	$P\bar{1}$	$P\bar{1}$	$P\bar{1}$	$Pna2_1$
a, Å	12.970(4)	13.4350(4)	12.3183(6)	12.794(1)	24.883(3)
b, Å	27.644(7)	13.5298(4)	12.6860(6)	15.129(1)	15.962(2)
c, Å	29.174(8)	17.9662(5)	22.7533(12)	18.119(1)	17.930(2)
α, deg		98.7273(11)	102.535(3)	73.841(1)	
β, deg	96.932(5)	106.3306(10)	94.787(3)	79.979(1)	
γ, deg		94.8176(11)	91.770(3)	89.871(1)	
V, Å^3	10383(5)	3069.99(15)	3454.4(3)	3313.1(4)	7127.7(15)
Z	4	2	2	2	4
D_{calcd}, g/cm^3	1.390	1.591	1.498	1.480	1.467
R, R_w[a]	0.066, 0.114	0.049, 0.060	0.051, 0.058	0.062, 0.164	0.068, 0.159
GOF	0.699	1.84	1.92	1.023	0.929

[a] See the Supporting Information for definitions of R and R_w.

the IR spectra are <2143 cm^{-1}. In addition, [TpRu(N_2)(PEt_3)$_2$][BPh_4] has been characterized with a Ru−N distance of 1.91(2) Å and a ν_{NN} = 2163 cm^{-1}.[48] [CpRu(N_2)(dippe)][BPh_4] and [Cp*Ru(N_2)(dippe)][BPh_4] (dippe = diisopropylphosphinoethane) have been isolated with ν_{NN} at 2145 and 2120 cm^{-1}, respectively.[49] The relatively long Ru−N bond distance and high-energy ν_{NN} of complex **4** could be due to the combination of a cationic charge and competition for Ru−N_2 π-back-donation with the strong π-acid CO. The high-energy ν_{NN} (2249 cm^{-1}) of complex **4** compared to similar Ru systems is consistent with the strong π-acid CO competing for metal dπ electrons. The combination of dinitrogen in the same coordination sphere with CO is rare.[50−52] Thus, we suggest that the Ru−N bond is relatively weak, a proposal that is consistent with the highly labile nature of the dinitrogen ligand of **4**. Several other late transition metal dinitrogen complexes with pincer ligands have also been reported with either monodentate η^1-N_2−M or M−μ-N_2−M coordination.[41,46,53−60]

Ligand Donor Ability and Agostic Interaction. The stability of complex **1** as a five-coordinate, 16-electron system could be due to the bulky *tert*-butyl groups, π stabilization provided by the chloride ligand, and/or the strong trans effect of the CO ligand. The coordination of a two-electron donor ligand results in the formation of a saturated 18-electron complex of the type (PCP)Ru(CO)(L)(Cl). For example, (PCP)Ru$(CO)_2$Cl and (PCP)Ru(CO)(PMe_3)Cl have been isolated and characterized;[25,28] however, (PCP)Ru(CO)(NCMe)Cl and (PCP)Ru(CO)(NH_3)Cl can only be observed in solution, with attempts to isolate them resulting in the dissociation of NCMe or NH_3.[24,25] The electron density of the metal center as influenced by the "X" ligands of systems of the type [(PCP)Ru(CO)(X)]$^{n+}$ (n = 0 or 1) can be approximated by the energy of the CO absorptions. In addition to the new systems reported herein, other complexes of the type (PCP)Ru(CO)(X) have been previously reported.[24,25,59,61] The CO absorption energies of a series of systems are listed in Table 2.

Table 2. CO Stretching Frequencies (cm^{-1}) for Complexes of the Type [(PCP)Ru(CO)(X)]$^{n+}$ (n = 0 or 1)

X	ν_{CO}	X	ν_{CO}	X	ν_{CO}
NH_2	1890	NHPh	1900	(PCP)(CO)Ru(Cl)	1939
Me	1893	H	1906	OTf	1941
OH	1896	C≡CPh	1915	η^1-$ClCH_2Cl$	1964
Ph	1900	Cl	1919	η^1-N_2	1987

Potentially, the unsaturated metal center of **1** could also be stabilized by a C−H agostic interaction.[62,63] Caulton et al. reported double agostic interactions for the 14-electron complex [Ru(Ph)(CO)(P^tBu_2Me)][BAr′$_4$] with an average Ru/$C_{agostic}$ distance of 2.87 Å.[14] In another case, the neutral 14-electron complex $RuCl_2${PPh_2(2,6-$Me_2C_6H_3$)}$_2$ with two agostic interactions with an average Ru/$C_{agostic}$ distance 2.65 Å has been reported.[16] There are several other unsaturated ruthenium complexes with a single C−H agostic interaction with Ru/$C_{agostic}$ distances less than 3 Å.[17−19,27,28,59] However, there is no agostic interaction reported for **1**, which is possibly due to the presence of the π-donating chloride ligand, which can stabilize the 16-electron ruthenium center;

(48) Tenorio, M. A. J.; Tenorio, M. J.; Puerta, M. C.; Valerga, P. *J. Chem. Soc., Dalton Trans.* **1998**, 3601−3608.
(49) de los Ríos, I.; Tenorio, M. J.; Padilla, J.; Puerta, M. C.; Valerga, P. *Organometallics* **1996**, *15*, 4565−4574.
(50) Luo, X.-L.; Kubas, G. J.; Burns, C. J.; Eckert, J. *Inorg. Chem.* **1994**, *33*, 5219−5229.
(51) Sato, M.; Tatsumi, T.; Kodama, T.; Hidai, M.; Uchida, T.; Uchida, Y. *J. Am. Chem. Soc.* **1978**, *100*, 4447−4452.
(52) Kandler, H.; Gauss, C.; Bidell, W.; Rosenberger, S.; Burgi, T.; Eremenko, I. L.; Veghini, D.; Orama, O.; Burger, P.; Berke, H. *Chem.−Eur. J.* **1995**, *1*, 541−548.
(53) van der Boom, M. E.; Milstein, D. *Chem. Rev.* **2003**, *103*, 1759−1792.
(54) van der Boom, M. E.; Liou, S.-Y.; Ben-David, Y.; Shimon, L. J. W.; Milstein, D. *J. Am. Chem. Soc.* **1998**, *120*, 6531−6541.
(55) Vigalok, A.; Ben-David, Y.; Milstein, D. *Organometallics* **1996**, *15*, 1839−1844.
(56) Vigalok, A.; Milstein, D. *Organometallics* **2000**, *19*, 2061−2064.
(57) Jensen, C. M. *Chem. Commun.* **1998**, 2443.
(58) Lee, D. W.; Kaska, W. C.; Jensen, C. M. *Organometallics* **1998**, *17*, 1.
(59) Gusev, D. G.; Dolgushin, F. M.; Antipin, M. Y. *Organometallics* **2000**, *19*, 3429−3434.
(60) Abbenhuis, R. A. T. M.; del Rio, I.; Bergshoef, M. M.; Boersma, J.; Veldman, N.; Spek, A. L.; van Koten, G. *Inorg. Chem.* **1998**, *37*, 1749−1758.
(61) Lail, M.; Bell, C. M.; Conner, D.; Cundari, T. R.; Gunnoe, T. B.; Petersen, J. L. *Organometallics* **2004**, *23*, 5007−5020.
(62) Brookhart, M.; Green, M. L. H.; Wong, L.-L. *Prog. Inorg. Chem.* **1988**, *36*, 1−124.
(63) Brookhart, M.; Green, M. L. H. *J. Organomet. Chem.* **1983**, *250*, 395−408.

however, for complexes **3** and **4** with the weak donating ligands CH_2Cl_2 or N_2, respectively, the unsaturated formal 16-electron metal centers are apparently each stabilized by a single agostic interaction. Milstein et al. have reported the agostic interaction for $[(PCP)Ru(CO)_2]^+$.[28] Thus, an agostic interaction appears favorable for systems of the type $[(PCP)Ru(CO)(L)]^{n+}$ ($n = 0$ or 1) in which "L" is either weakly coordinating or a strong π-acid. In contrast, for L = Cl, the formation of a sixth Ru−ligand bond does not appear to be highly favorable; hence, an agostic interaction is not observed and ligands such as NH_3, NCMe, and PMe_3 very weakly coordinate to the (PCP)Ru(CO)(Cl) system (see above).

Density Functional Theory (DFT) Calculations for Comparison of $[(PCP)Ru(CO)(L)]^+$ (L = η^1-$ClCH_2Cl$, η^1-N_2, η^1-FC_6H_5, or Agostic) Complexes. Hybrid mixed quantum mechanics/molecular mechanics (QM/MM) calculations on full experimental models were performed for the comparison of the binding of weak bases to $[(PCP)Ru(CO)]^+$ to form $[(PCP)Ru(CO)(L)]^+$ (L = η^1-$ClCH_2Cl$, η^1-N_2, η^1-FC_6H_5, or C−H agostic). For the four-coordinate, 14-electron complex $[(PCP)Ru(CO)]^+$, both agostic and nonagostic conformers were investigated. Three of the *tert*-butyl groups were modeled classically (using MM); the one with an agostic interaction was modeled at the same B3LYP/CEP-31G(d) level of theory as the other quantum atoms. Although geometry optimizations were started from crystallographic coordinates, it must be noted that an extensive conformational analysis of these species was not performed and the reported energetics must be viewed in this light. Upon geometry optimization, the complex $[(PCP)Ru(CO)]^+$ had one weak agostic interaction with a distance $Ru\cdots C_{agostic} = 3.25$ Å as well as a compressed bond angle, Ru−P−C = 102.1°. The small Ru−P−C bond angle is akin to that noted in the crystal structures of the agostic interactions for $[(PCP)Ru(CO)(L)]^+$ complexes (see above). In terms of the calculated binding energy, the agostic conformer is 6 kcal/mol more stable than the nonagostic conformer (Figure 4).

For the five-coordinate, 16-electron complexes $[(PCP)Ru(CO)(L)]^+$, binding of the fifth ligand to the nonagostic conformer of $[(PCP)Ru(CO)]^+$ afforded nonagostic complexes with the following calculated binding energies: ΔE (kcal/mol) = −12 (L = η^1-CH_2Cl_2), −13 (L = FC_6H_5), and −18 (L = η^1-N_2) (Figure 4). An agostic conformer for these five-coordinate complexes was found for two of the ligands (L = CH_2Cl_2, FC_6H_5) although none could be found for L = N_2. Manually altering the geometry to create agostic interactions resulted in optimized geometries in which this interaction was absent. Each of the agostic conformers of $[(PCP)Ru(CO)(L)]^+$, with L = CH_2Cl_2 and FC_6H_5, had one agostic interaction with calculated distances $Ru\cdots C_{agostic}$ = 3.20 and 3.22 Å, respectively.

The relative order for the $[(PCP)Ru(CO)]^+$ and $[(PCP)Ru(CO)(L)]^+$ complexes in terms of increasing binding energy is $CH_{agostic} < CH_2Cl_2 \sim PhF < N_2$. The same order is seen in full QM calculations on small models (i.e., PCP → PCP′, where *tert*-butyl groups are replaced by hydrogen). Additionally, binding energies for PCP′ models are of the same magnitude (±1−2 kcal/mol), implying that steric factors play a secondary role in discrimination among the various bases for coordination to ruthenium. The calculations, thus, support the experimental inference made above that fluorobenzene is a competent base for $[(PCP)Ru(CO)(L)]^+$ and that a 14-electron, four-coordinate species $[(PCP)Ru(CO)]^+$ (both agostic and nonagostic conformers) represents a higher energy state than $[(PCP)Ru(CO)(L)]^+$ for L = η^1-N_2, η^1-CH_2Cl_2, or PhF (Figure 4).

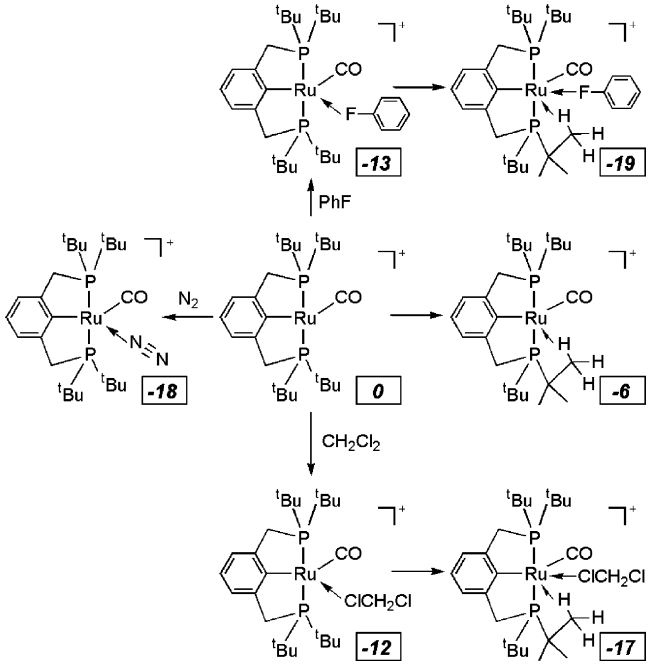

Figure 4. QM/MM (B3LYP/CEP-31G(d):UFF) binding energies in kcal/mol (given in boxes) relative to the nonagostic isomer of $[(PCP)Ru(CO)]^+$.

Geometry optimization, followed by vibrational frequency analysis, was performed on truncated 16-electron $[(PCP')Ru(CO)(L)]^+$ models to ascertain their CO absorptions. The experimental order of ν_{CO} (cm^{-1}) for $[(PCP)Ru(CO)(L)]^+$ is 1987 (L = η^1-N_2), 1964 (L = η^1-CH_2Cl_2), and 1953 (L = PhF) with the latter being inferred from equilibrium studies; the calculated ν_{CO} (cm^{-1}) values for the corresponding PCP′ models are 2085, 2066, and 2054. Scaling the calculated CO stretching frequencies by a typical factor of 0.95 yields ν_{CO} = 1981 cm^{-1} (L = η^1-N_2), 1963 cm^{-1} (L = η^1-CH_2Cl_2), and 1951 cm^{-1} (L = PhF) for $[(PCP')Ru(CO)(L)]^+$. The proposed fluorobenzene complex, **5**, has an experimental ν_{CO} of 1953 cm^{-1}. Thus, the calculations support the intermediacy of a fluorobenzene complex in the solution equilibrium experiments.

The computational studies suggest that the weakly coordinating ligands η^1-N_2, η^1-CH_2Cl_2, and PhF are preferred over the four-coordinate complex $[(PCP)Ru(CO)]^+$ with or without an agostic interaction, and these calculations are consistent with experimental observations. The calculations also indicate that the agostic fragment $[(PCP)Ru(CO)]^+$ has little preference for binding of η^1-N_2, η^1-CH_2Cl_2, or PhF with calculated differences in energies of only 1 kcal/mol (Figure 4).

Reaction of 3 with $PhCHN_2$. The labile CH_2Cl_2 ligand of complex **3** makes it a potentially useful synthetic precur-

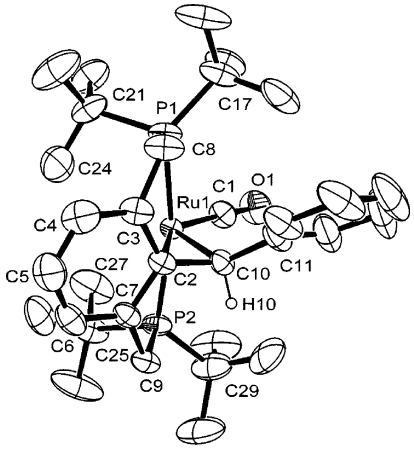

Figure 5. ORTEP diagram (30% probability) of [(PCP−CHPh)Ru(CO)][BAr′$_4$] (**7**) (hydrogen atoms, except the one on "PhC*H*", and the BAr′$_4$ counterion have been omitted for clarity). Selected bond lengths (Å) and bond angles (deg): Ru1−C2, 2.329(8); Ru1−C10, 2.11(1); C2−C10, 1.47(1); C2−C3, 1.42(1); C2−C7, 1.42(1); C3−C4, 1.37(2); C4−C5, 1.36(2); C5−C6, 1.36(2); C6−C7, 1.398(1); C2−Ru1−C10, 38.2(3); C2−Ru1−C1, 141.9(4); P1−Ru1−P2, 164.86(9); Ru1−C10−C2, 79.2(6); Ru1−C10−C11, 128.8(6); C11−C10−C(2), 124.2(9); C10−C2−Ru1, 62.6(5).

sor. A pentane solution of excess phenyldiazomethane, $PhCHN_2$, was added to a CH_2Cl_2 solution of **3**. A single ruthenium product was isolated after workup in 80% yield and was fully characterized by ^{1}H, ^{31}P, ^{19}F, and ^{13}C NMR and IR spectroscopy, elemental analysis, and a single-crystal X-ray diffraction study. Spectral data do not provide evidence for the presence of a benzylidene ligand, as a resonance downfield of 10 ppm in the ^{1}H NMR spectrum, which would be consistent with a carbene proton, is not observed nor is a resonance consistent with a carbene carbon observed in the ^{13}C NMR spectrum. Four doublets with $J_{PH} = 14$ Hz are observed in the region of 0.8−1.6 ppm in the ^{1}H NMR spectrum, which can be assigned as *tert*-butyl groups. Two doublets at 46.2 and 23.6 ppm with $J_{PP} = 218$ Hz are present in the ^{31}P{^{1}H} NMR spectrum. An absorption due to the CO ligand is observed at 1931 cm^{-1} in the IR spectrum.

A solid-state X-ray crystal structure analysis was performed and revealed the product as [(PCP−CHPh)Ru(CO)][BAr′$_4$] (PCP−CHPh = κ^4-*P*,*P*,*C*,*C*-1-CHPh-2,6-$(CH_2P^tBu_2)_2$−C_6H_3) (**7**) (Figure 5). Thus, rather than formation of a stable and isolable ruthenium alkylidene complex, the coupling of the carbene moiety "CHPh" with the PCP ipso carbon occurs. Prominent geometric features include a C2−Ru1−C1 bond angle of 141.9(4)° and a single *weak* agostic interaction (Ru1−C24, 3.06 Å). The Ru1−C2 bond distance (2.329(8) Å) is longer than typical Ru−C_{ipso} bond distances (e.g., 2.053(3) Å in complex **3**). The C2−C10 bond distance (1.47(1) Å) is slightly shorter than a carbon−carbon single bond (∼1.54 Å) but longer than a carbon−carbon double bond (∼1.34 Å). No evidence for possible η^3-allyl or η^4-diene coordination involving the PCP phenyl ring or carbene phenyl ring is observed.[64,65] All distances between Ru and

Scheme 2. Comparison of Bond Lengths (Å) of C_6-Ring Moieties of Complexes **4**, **7**, and **8** and Assignment of σ-Arenium for Complexes **7** and **8**[a]

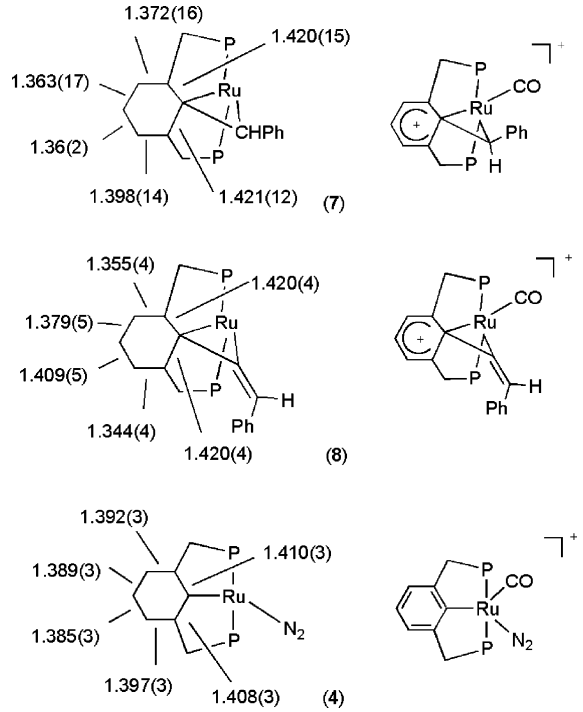

[a] The left side shows bond length data, and the right side shows structure assignments.

other phenyl carbons are longer than 3 Å. These bonding interactions have an effect on the aromaticity of the PCP phenyl ring with the best description being an arenium moiety based on the bond length analysis (Scheme 2). The bond lengths of C2−C3 (1.42(1) Å) and C2−C7 (1.42(1) Å) are slightly longer (∼0.06 Å) than those of C5−C6 (1.36(2) Å) and C4−C5 (1.36(2) Å). In contrast, a smaller difference was observed in complex **4** (∼0.02 Å). The C−C bond length in benzene is 1.394(5) Å.[66] Similar structures such as σ-arenium complexes of Pt, Ir, or Rh and methylene arenium complexes of Ir or Rh have been reported.[53,67−70]

A possible mechanism for the conversion of **3** and $PhCHN_2$ to **7** involves the initial formation of a Ru benzylidene complex followed by an intramolecular C−C coupling sequence (Scheme 3). If this pathway is operative, complex **7** is a trapped intermediate of a formal insertion of a carbene ligand into a Ru−aryl bond. Similar transformations are important C−C bond forming reactions.[71−74] Hybrid QM/MM calculations on full experimental models suggest

(64) Jordan, R. F.; LaPointe, R. E.; Bajgur, C. S.; Echols, S. F.; Willett, R. *J. Am. Chem. Soc.* **1987**, *109*, 4111−4113.
(65) Mintz, E. A.; Moloy, K. G.; Marks, T. J.; Day, V. W. *J. Am. Chem. Soc.* **1982**, *104*, 4692−4695.
(66) Schomaker, V.; Pauling, L. *J. Am. Chem. Soc.* **1939**, *61*, 1769−1780.
(67) Albrecht, M.; van Koten, G. *Angew. Chem., Int. Ed.* **2001**, *40*, 3750−3781.
(68) Terheijiden, J.; van Koten, G.; Vinke, I. C.; Spek, A. L. *J. Am. Chem. Soc.* **1985**, *107*, 2891−2898.
(69) Vigalok, A.; Shimon, L. J. W.; Milstein, D. *J. Am. Chem. Soc.* **1998**, *120*, 477−483.
(70) Vigalok, A.; Rybtchinski, B.; Shimon, L. J. W.; Ben-David, Y.; Milstein, D. *Organometallics* **1999**, *18*, 895−905.
(71) Hoover, J. F.; Stryker, J. M. *J. Am. Chem. Soc.* **1990**, *112*, 464−465.
(72) Bergamini, P.; Costa, E.; Cramer, P.; Hogg, J.; Orpen, A. G.; Pringle, P. G. *Organometallics* **1994**, *13*, 1058−1060.
(73) Trace, R. L.; Sanchez, J.; Yang, J.; Yin, J.; Jones, W. M. *Organometallics* **1992**, *11*, 1440−1442.
(74) Tan, K. L.; Bergman, R. G.; Ellman, J. A. *J. Am. Chem. Soc.* **2002**, *124*, 3202−3203.

Scheme 3. Proposed Reaction Pathway of $[(PCP)Ru(CO)(\eta^1\text{-}ClCH_2Cl)]^+$ (**3**) with $PhCHN_2$ To Form $[(PCP-CHPh)Ru(CO)]^+$ (**7**)

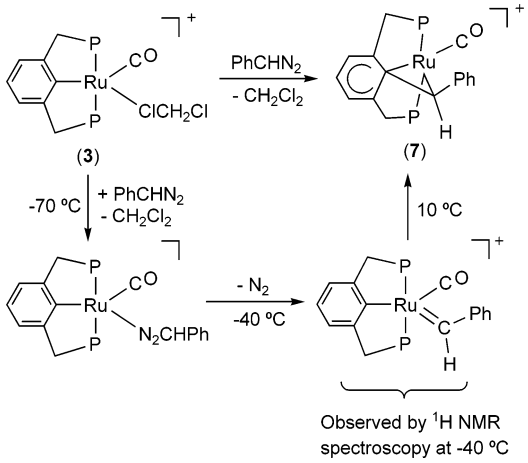

that this reaction is exothermic by more than 30 kcal/mol; other computational studies relevant to this transformation are given below. In an effort to experimentally observe reaction intermediates for the conversion of **3** to **7**, we monitored the reaction of **3** and $PhCHN_2$ using variable temperature ^1H NMR spectroscopy in CD_2Cl_2. Complex **3** and $PhCHN_2$ were dissolved in CD_2Cl_2 at −70 °C and transferred to an NMR probe precooled to this temperature. At −70 °C, there was no observation of a downfield resonance that would be diagnostic of the formation of a benzylidene complex; however, complex **3** was converted to a new complex that is likely a ruthenium diazophenylmethane complex. The temperature of the NMR probe was incrementally increased to room temperature. At −40 °C, a decrease in the intensity of resonances due to **3** is observed, and the formation of a resonance at 26.0 ppm (^1H NMR) occurs. This downfield resonance most likely indicates the formation of the benzylidene complex $[(PCP)(CO)Ru{=}CHPh][BAr'_4]$. At 10 °C, the resonance due to the putative carbene complex disappears and the quantitative formation of complex **7** is observed. These results suggest that **7** is formed from an intermediate carbene complex rather than direct attack of N_2CHPh on the Ru−aryl moiety. Rhodium benzylidene complexes with a pincer ligand have been synthesized from the reaction of phenyldiazomethane with rhodium dinitrogen precursors, although no carbene insertion reaction has been reported for the Rh benzylidene complex.[53,56,75] For example, the benzylidene complex $(PCP^{Me2})Rh{=}CHPh$ is isolable (PCP^{Me2} = 2,6-$(CH_2P^tBu_2)_2$-3,5-$Me_2-C_6H_1$). The difference in reactivity with phenyldiazomethane between the PCP−Ru system reported herein and the Rh systems may be derived from the ability of the Rh(I) complexes to stabilize (kinetically and/or thermodynamically) the benzylidene moiety through metal-to-ligand π-back-bonding. Evidence of increased π-back-bonding ability for the Rh systems versus the Ru fragment discussed herein is apparent from the relative ν_{NN} of the dinitrogen complexes $(PCP^{Me2})Rh(N_2)$ (2120 cm^{-1}) and $[(PCP)Ru(CO)(N_2)]^+$ (2249 cm^{-1}). It is also feasible to consider that the preferred square planar geometry of four-coordinate Rh(I) inhibits the C−C bond formation step.

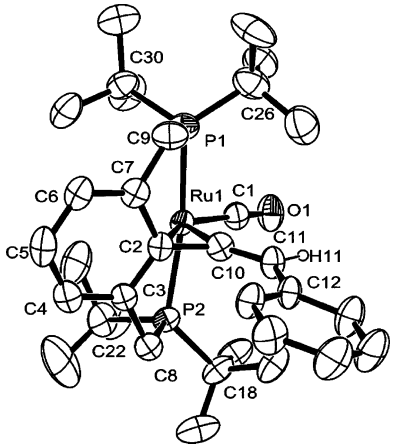

Figure 6. ORTEP diagram (30% probability) of $[(PCP-CCHPh)Ru(CO)][BAr'_4]$ (**8**) (hydrogen atoms, except the "C(Ph)*H*" hydrogen, and the BAr'_4 counterion have been omitted for clarity). Selected bond length (Å) and bond angles (deg): Ru1−C2, 2.352(2); Ru1−C10, 1.980(2); C2−C10, 1.466(5); C10−C11, 1.316(4); C2−C3, 1.420(4); C2−C7, 1.420(4); C3−C4, 1.355(4); C4−C5, 1.379(5); C5−C6, 1.409(5); C6−C7, 1.344(4); C2−C10−C11, 134.7(3); C10−C11−C12, 127.1(3); C2−Ru1−C10, 38.3(1); C2−Ru1−C1, 144.5(1); P1−Ru1−P2, 166.1(1).

Reaction of 3 with PhC≡CH. The formation of vinylidene ligands from reaction of transition metal systems with terminal acetylenes is known.[76] To determine if the vinylidene−C_{ipso} coupling reaction occurs as observed for the formation of **7**, the reaction of **3** with phenylacetylene in CD_2Cl_2 was monitored by NMR spectroscopy. The combination of **3** and PhC≡CH results in an immediate color change from orange to green and the formation of a new complex, as indicated by two new virtual triplets at 1.62 and 1.10 ppm in the ^1H NMR spectrum and a singlet at 31.5 ppm in ^{31}P NMR spectrum. In addition, a triplet at 6.55 ppm with a coupling constant of J = 3 Hz is observed by ^1H NMR spectroscopy. This complex undergoes slow transformation to a new product with complete conversion observed by NMR spectroscopy after 3−4 days at room temperature. Two new virtual triplets at 1.43 and 1.20 ppm and a broad singlet at 5.87 ppm are present in the ^1H NMR spectrum of the final product, and a new singlet at 37.4 ppm is observed in the ^{31}P NMR spectrum. This ultimate product is likely a result of a vinylidene−C_{ipso} coupling to yield $[(PCP-C{=}CHPh)Ru(CO)][BAr'_4]$ (PCP−C=CHPh = κ^4-*P*,*P*,*C*,*C*-1-(C=CHPh)-2,6-$(CH_2P^tBu_2)_2-C_6H_3$) (**8**). The structure of **8** is similar to that of **7** (Figure 6). However, the phenyl ring of the {C=CHPh} fragment resides in a plane of mirror symmetry that renders the two phosphine groups symmetry equivalent. In contrast, the CHPh group is in a perpendicular orientation for complex **7**, which results in two symmetry unique phosphines. Thus, four *tert*-butyl groups are observed as four doublets for **7**, while only two virtual triplets were observed for **8** by ^1H NMR spectroscopy. Likewise, two resonances are observed for **7** and a single resonance is observed for **8** by ^{31}P NMR spectroscopy.

(75) Cohen, R.; Rybtchinski, B.; Gandelman, M.; Rozenberg, H.; Martin, J. M. L.; Milstein, D. *J. Am. Chem. Soc.* **2003**, *125*, 6532−6546.

(76) Bruce, M. I. *Chem. Rev.* **1991**, *91*, 197−257.

Jia et al. and Gusev et al. have reported similar coupling reactions of terminal acetylenes with ruthenium pincer complexes.[77−79] However, reaction of terminal acetylenes with osmium derivatives resulted in isolable vinylidene complexes.[79,80] For the reaction of (PCP−Ph)Ru(PPh_3)(Cl) (PCP−Ph = 2,6-$(CH_2PPh_2)_2C_6H_3$) with PhC≡CH, Jia et al. discussed the mechanism as proceeding via alkyne coordination, transformation to a vinylidene complex followed by the C−C coupling step to form the product. Neither the proposed alkyne-coordinated intermediate nor the vinylidene complex has been observed.[77,78] In contrast, an intermediate Ru complex is observed for the reaction of **3** with PhC≡CH to form **8**, and likely identities of this system are the η^2-alkyne complex [(PCP)Ru(CO)(η^2-PhCCH)][BAr'_4] or the vinylidene complex [(PCP)(CO)Ru=C=CHPh][BAr'_4]. The observed intermediate is unlikely a Ru hydride−alkynyl complex, since the anticipated upfield resonance due to a hydrido ligand is not observed. No resonance downfield of 200 ppm, except a triplet at 208.5 ppm due to CO, is observed in the ^{13}C NMR spectrum, which provides evidence against the presence of a vinylidene intermediate; however, due to likely C−P coupling and relaxation, the intensity of this resonance is anticipated to be weak and difficult to observe. Thus, the absence of an assignable vinylidene carbon resonance is not sufficient evidence to conclusively assign the identity of the intermediate. On the basis of DFT calculations (see below), we suggest that the intermediate is the vinylidene complex [(PCP)(CO)Ru=C=CHPh][BAr'_4]; however, the inability to cleanly isolate and grow crystals of this system precludes a definitive conclusion based solely on experimental data.

The reactions of phenylacetylene with five-coordinate complexes **1** or **6** were studied to determine if the weakly bound CH_2Cl_2 of **3** is necessary to observe the formation of **8**. Reaction of triflate complex **6** with PhC≡CH yields similar results as observed for complex **3**, including the formation of an intermediate and the eventual conversion to the final coupling product, **8**, albeit the total reaction time is ∼10 days at room temperature compared to ∼3 days starting from complex **3**. In contrast, there is no observable reaction between chloride complex **1** and PhC≡CH at room temperature after 7 days.

DFT Calculations on the Formation of Complexes 7 and 8. The formation of complexes **7** and **8** was probed using similar computational methodologies to those described above. Given the difficulties in isolating appropriate transition states for carbene (and vinylidene) insertion, the corresponding DFT calculations on truncated PCP′ models (vide supra) were also performed. Calculations support the experimental inference about the intermediacy of terminal [(PCP)(CO)-Ru=$(C)_{0,1}$=CHPh]$^+$ complexes, as both species are found to be stable minima. Furthermore, the insertion reactions are found to be thermodynamically feasible: $\Delta E = -8$ kcal/mol for =C(H)Ph insertion to form **7** and −27 kcal/mol for =C=C(H)Ph insertion to form **8** (Figure 7). The corresponding enthalpy values for truncated PCP′ models are −17 kcal/mol (carbene insertion) and −22 kcal/mol (vinylidene insertion). These QM energetics on small models, combined with the analysis of the QM portion of the QM/MM extrapolated energies, suggest that the difference in the energetics of carbene and vinylidene has both electronic and steric components. Interestingly, the carbene insertion is retarded (∼4−5 kcal/mol) by steric factors, while the vinylidene insertion is facilitated by a comparable amount by steric factors. Presumably, this is a reflection of the extra carbon atom of the vinylidene minimizing steric hindrance between the phenyl substituent and the phosphine *tert*-butyl groups of complex **8** as compared with complex **7**.

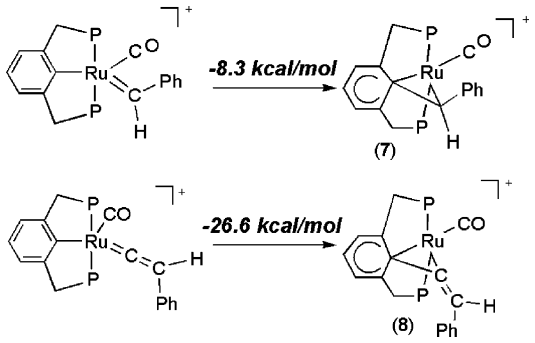

Figure 7. Calculated ONIOM reaction energies in kcal/mol.

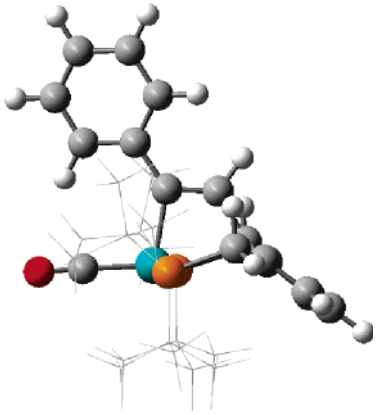

Figure 8. Calculated structure of the product from insertion of the alkyne into the PCP ligand starting from [(PCP)(CO)Ru(η^2-HC≡CPh)]$^+$. Some atoms of the PCP ligand are shown in wire frame for clarity.

A terminal alkyne complex as a possible intermediate in the formation of **8** was probed through QM/MM calculations. Construction of [(PCP)(CO)Ru(η^2-HC≡CPh)]$^+$ (alkyne in the equatorial plane) followed by geometry optimization yielded a high energy intermediate (ca. 13 kcal/mol above **8**) corresponding to the insertion of the alkyne triple bond into the Ru−C_{ipso} of the PCP ligand (Figure 8). Model calculations on [(PCP′)(CO)Ru(η^2-HC≡CH)]$^+$ yielded a stationary point, but this species was a transition state with the imaginary frequency corresponding to the rotation of the acetylene ligand to a conformation with the C≡C bond perpendicular to the equatorial plane, which is 23 kcal/mol

(77) Lee, H. M.; Yao, J.; Jia, G. *Organometallics* **1997**, *16*, 3927.
(78) Jia, G.; Lee, H. M.; Xia, H. P.; Williams, I. D. *Organometallics* **1996**, *15*, 5453.
(79) Gusev, D. G.; Maxwell, T.; Dolgushin, F. M.; Lyssenko, M.; Lough, A. J. *Organometallics* **2002**, *21*, 1095−1100.
(80) Wen, T. B.; Cheung, Y. K.; Yao, J.; Wong, W.-T.; Zhou, Z. Y.; Jia, G. *Organometallics* **2000**, *19*, 3803−3809.

Scheme 4. Reaction of $[(PCP)Ru(CO)(\eta^1\text{-}ClCH_2Cl)]^+$ (**3**) with PhC≡CH To Yield the Coupling Product via an Observable Intermediate Proposed To Be the Vinylidene Complex $[(PCP)(CO)Ru{=}C{=}CHPh]^+$

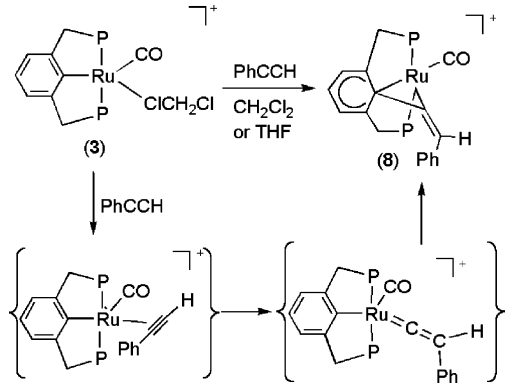

higher in energy than the vinylidene model $[(PCP')(CO)Ru{=}C{=}CH_2]^+$. Such a perpendicular conformation for the experimental $[(PCP)(CO)Ru(\eta^2\text{-}HC{\equiv}CPh)]^+$ seems even less plausible on steric grounds, given the expected steric repulsion between the Ph and the *tert*-butyl groups. (See Table 1 for crystallographic data and parameters for complexes **2**, **3**, **4**, **7**, and **8**.)

Summary

The 14-electron fragment $[(PCP)Ru(CO)]^+$ appears to bind weakly coordinating ligands such as dinitrogen, methylene chloride, and fluorobenzene in preference to formation of agostic interactions. This suggestion is supported by both experimental observations and calculations. The reaction of $[(PCP)Ru(CO)(\eta^1\text{-}ClCH_2Cl)][BAr'_4]$ (**3**) with N_2CHPh or phenylacetylene results in transformations involving the C−C bond formation of the PCP phenyl ring. Experimental studies suggest that the reaction with N_2CHPh proceeds via the formation of a Ru benzylidene complex and that an intermediate vinylidene complex may be central to the reaction with phenylacetylene. The QM/MM calculations on $[(PCP)(CO)Ru{=}(C)_{0,1}{=}CHPh]^+$ and the DFT calculations on $[(PCP')(CO)Ru{=}(C)_{0,1}{=}CH_2]^+$ provide support for the thermodynamic feasibility of the experimental mechanisms leading to **7** (Scheme 3) and **8** (Scheme 4).

Experimental Section

General Methods. Unless otherwise noted, all procedures were performed under an atmosphere of dinitrogen in a glovebox or using standard Schlenk techniques. Oxygen levels were <15 ppm for all glovebox manipulations. Pentane and fluorobenzene were distilled from P_2O_5. Methylene chloride was purchased as an OptiDry solvent (<50 ppm H_2O), passed through two columns of activated alumina, and then distilled over CaH_2 prior to use. CD_2Cl_2 and $CDCl_3$ were degassed via three freeze−pump−thaw cycles and stored over 4 Å molecular sieves. ^1H and ^{13}C NMR measurements were performed on a Varian Mercury 300 or 400 MHz spectrometer and referenced to tetramethylsilane (TMS) using resonances due to residual protons in the deuterated solvents or the ^{13}C resonances of the deuterated solvents. All ^{31}P NMR spectra were recorded on a Varian Mercury instrument operating at a frequency of 161 MHz with 85% phosphoric acid (0 ppm) as the external standard. All ^{19}F spectra were recorded on a Varian Mercury instrument operating at a frequency of 376.5 MHz with CF_3CO_2H (−78.5 ppm) as the external standard. IR spectra were acquired of solutions in KBr solvent cells using a Mattson Genesis II FT-IR instrument. Elemental analyses were conducted by Atlantic Microlab, Inc. (PCP)Ru(CO)(Cl) (**1**), (PCP)Ru(CO)(OTf) (**6**), phenyldiazomethane, and $NaBAr'_4$ were synthesized as previously reported.[25,27,81,82] Phenylacetylene was purchased from a commercial source and used without further purification.

$[\{(PCP)Ru(CO)\}_2(\mu\text{-}Cl)][BAr'_4]$ (2). (PCP)Ru(CO)(Cl) (**1**) (0.225 g, 0.403 mmol) was dissolved in approximately 20 mL of CH_2Cl_2, and 0.5 equiv of $NaBAr'_4$ (0.200 g, 0.220 mmol) was added. After stirring for 30 min, the color changed from brown to dark red and the CO absorption changed from 1920 to 1939 cm^{-1}, as monitored by IR spectroscopy. After vacuum filtration through a fine porosity frit, the filtrate was concentrated to 1−2 mL and 10 mL of hexanes was added to yield an orange solid. The solid was collected with a fine porosity frit, washed with hexanes, and dried in vacuo (0.310 g, 0.160 mmol, 80%). Crystals suitable for an X-ray diffraction study were obtained by slow diffusion of pentane into a CH_2Cl_2 solution of **2** at −20 °C. IR (CH_2Cl_2 solution): ν_{CO} = 1939 cm^{-1}. ^1H NMR ($CDCl_3$, δ): 7.71 (8H, br s, BAr'_4 phenyl), 7.52 (4H, br s, BAr'_4 phenyl), 7.16 (4H, m, PCP phenyl), 7.02 (2H, m, PCP phenyl), 3.45 (8H, m, PCP CH_2), 1.74−0.85 (∼72H, overlapping multiplets, PCP CH_3). $^{31}P\{^1H\}$ NMR ($CDCl_3$, δ): 74.1 (d, J_{PP} = 228 Hz), 68.9 (d, J_{PP} = 228 Hz). ^{19}F NMR ($CDCl_3$, δ): −63.0. Anal. Calc for $C_{82}H_{98}BClF_{24}O_2P_4Ru_2$: C, 50.67; H, 5.08. Found: C, 50.16; H, 4.85.

$[(PCP)Ru(CO)(\eta^1\text{-}ClCH_2Cl)][BAr'_4]$ (3). (PCP)Ru(CO)(OTf) (**6**) (0.100 g, 0.149 mmol) was dissolved in 10 mL of CH_2Cl_2, and approximately 1 equiv of $NaBAr'_4$ (0.140 g, 0.158 mmol) was added. After stirring for 30 min, the color changed from brown to orange and the CO absorption changed from 1941 to 1964 cm^{-1}, as monitored by IR spectroscopy. The solution was filtered through a fine porosity frit, and the filtrate was concentrated to 1 mL under reduced pressure. Approximately 10 mL of pentane was added, and the formation of an orange precipitate was noted. Upon filtration through a fine porosity frit, the solid was washed with pentane and dried in vacuo (0.180 g, 0.122 mmol, 82%). Crystals suitable for an X-ray diffraction study were obtained by slow diffusion of pentane into a CH_2Cl_2 solution of **3** at −20 °C. IR (CH_2Cl_2 solution): ν_{CO} = 1964 cm^{-1}. ^1H NMR (CD_2Cl_2, δ): 7.74 (8H, br s, BAr'_4 phenyl), 7.58 (4H, br s, BAr'_4 phenyl), 7.23 (2H, d, J_{HH} = 8 Hz, phenyl), 7.02 (1H, t, J_{HH} = 8 Hz, PCP phenyl), 5.35 (2H, s, free CH_2Cl_2), 3.50 (4H, m, PCP CH_2), 1.50 (18H, vt, N = 15 Hz, PCP CH_3), 1.11 (18H, vt, N = 15 Hz, PCP CH_3). $^{31}P\{^1H\}$ NMR (CD_2Cl_2, δ): 71.0 (br s). ^{19}F NMR (CD_2Cl_2, δ): −63.0. This compound is extremely air and moisture sensitive. Thus, elemental analysis was not obtained.

$[(PCP)Ru(CO)(\eta^1\text{-}N_2)][BAr'_4]$ (4). In a 25 mL round-bottom flask, (PCP)Ru(CO)(OTf) (**6**) (0.030 g, 0.045 mmol) was dissolved in 5−10 mL of fluorobenzene. Approximately 1 equiv of $NaBAr'_4$ was added, and the reaction progress was monitored by IR spectroscopy. After 30 min, the CO absorption (1944 cm^{-1}) due to the starting material had disappeared, and a major absorption at 1987 cm^{-1} was accompanied by a small side peak at 1953 cm^{-1}. In addition, an absorption at 2249 cm^{-1} was observed. The solution was stirred for approximately 3 h, during which time the IR spectrum did not change significantly. The solution was filtered

(81) Brookhart, M.; Grant, B.; Volpe, A. F., Jr. *Organometallics* **1992**, *11*, 3920−3922.
(82) Creary, X. *Organic Synthesis*; Wiley: New York, 1990; Collect. Vol. No. VII, p 438.

through a fine porosity frit, and the filtrate was transferred to a glass tube. After dilution with fluorobenzene, pentane was layered on top of the solution. Slow diffusion at −20 °C yielded orange needle crystals. A single crystal was selected for X-ray diffraction analysis.

[(PCP)Ru(CO)(FC_6H_5)][BAr'_4] (5). The preparation procedure was similar to that for complex **4**. After addition of $NaBAr'_4$ and upon observation of equilibrium by IR spectroscopy, the solution was purged with argon for 10 min. The peaks at 1987 cm^{-1} due to one CO absorption and at 2249 cm^{-1} due to N_2 absorption disappeared, and only one CO frequency at 1953 cm^{-1} was observed. The solution was purged with dinitrogen, and the absorptions at 1987 and 2249 cm^{-1} appeared with the side peak at 1953 cm^{-1}. The solution was then filtered through a fine porosity frit, and the filtrate was transferred to a glass tube and diluted with fluorobenzene. Repeated attempts to grow crystals resulted in decomposition upon removal of crystals from the solvent.

[(PCP−CHPh)Ru(CO)][BAr'_4] (7). [(PCP)Ru(CO)(η^1-CH_2Cl_2)]-[BAr'_4] (**3**) (0.150 g, 0.102 mmol) was dissolved in 15 mL of CH_2Cl_2. A red solution of excess $PhCHN_2$ in pentane was added. The resulting solution was stirred for 30 min, during which time the color changed from orange to pink. The solution was concentrated to approximately 5 mL under reduced pressure, and 10 mL of pentane was added to yield a pink precipitate. The solid was collected by vacuum filtration, washed with pentane, and dried in vacuo (0.120 g, 0.081 mmol, 80%). Crystals suitable for an X-ray diffraction study were obtained by slow diffusion of pentane into a CH_2Cl_2 solution of **7** at −20 °C. IR (CH_2Cl_2 solution): ν_{CO} = 1931 cm^{-1}. ^{1}H NMR (CD_2Cl_2, δ): 8.65 (1H, s, PhC*H*), 7.88 (2H, t, J_{HH} = 7 Hz), 7.73 (8H, br s, BAr'_4 phenyl), 7.57 (4H, br s, BAr'_4 phenyl), 7.50−7.12 (∼5H, overlapping multiplets, phenyl), 6.38 (1H, t, J_{HH} = 8 Hz, phenyl), 3.90 (1H, m, PCP CH_2), 3.68 (1H, m, PCP CH_2), 3.23 (1H, m, PCP CH_2), 2.98 (1H, m, PCP CH_2), 1.55 (9H, d, J_{PH} = 14 Hz, PCP CH_3), 1.18 (9H, d, J_{PH} = 14 Hz, PCP CH_3), 0.90 (9H, d, J_{PH} = 14 Hz, PCP CH_3), 0.86 (9H, d, J_{PH} = 14 Hz, PCP CH_3). ^{13}C{^{1}H} NMR ($CDCl_3$, δ): 202.8 (t, J_{PC} = 12 Hz, *C*O), 162.0 (m, J_{BC} = 50 Hz, B−C_{ipso}), 147.2−117.7 (multiple resonances due to aromatic carbons and *C*F_3), 44.4, 35.5 (each a d, J_{PC} = 15 Hz, PCP *C*H_2), 41.7 (br s, Ru−*C*HPh), 37.1 (m, PCP *C*Me_3), 30.8, 29.3, 29.1, 28.2 (each a d, J_{PC} = 4 Hz, PCP *C*H_3). ^{31}P{^{1}H} NMR (CD_2Cl_2, δ): 46.2 (d, J_{PP} = 218 Hz), 23.6 (d, J_{PP} = 218 Hz). ^{19}F NMR (CD_2Cl_2, δ): −63.2. Anal. Calc for $C_{64}H_{61}BF_{24}OP_2Ru$: C, 52.08; H, 4.17. Found: C, 52.67; H, 4.07.

Variable Temperature ^{1}H NMR Study of the Reaction of [(PCP)Ru(CO)(η^1-$ClCH_2Cl$)][BAr'_4] (3) with $PhCHN_2$. An NMR tube was charged with approximately 20 mg of [(PCP)Ru(CO)-(η^1-CH_2Cl_2)][BAr'_4] (**3**) in 0.7 mL of CD_2Cl_2 and cooled to −70 °C in an acetone/dry ice bath. Approximately 3 equiv of $PhCHN_2$ was added via syringe with an immediate color change from brown to red. The reaction mixture was transferred to an NMR probe cooled to −70 °C and was monitored by ^{1}H NMR spectroscopy as the temperature was incrementally increased to 25 °C. At −70 °C, there was no observation of a downfield resonance that would be diagnostic of the formation of a benzylidene complex; however, complex **3** was converted to a new complex that is likely a ruthenium diazophenylmethane complex. At −40 °C, a broad resonance was observed at 26.0 ppm (^{1}H NMR) that is consistent with the formation of [(PCP)(CO)Ru=CHPh][BAr'_4]. At 10 °C, the carbene resonance disappears and complete conversion to complex **7** is observed. The NMR resonances other than that assigned as being due to the putative ruthenium carbene hydrogen have not been assigned due to the complication of NMR spectra.

[(PCP−CCHPh)Ru(CO)][BAr'_4] (8). (A) Method A. [(PCP)-Ru(CO)(η^1-CH_2Cl_2)][BAr'_4] (**3**) (0.100 g, 0.068 mmol) was dissolved in 10 mL of CH_2Cl_2. Excess phenylacetylene (0.030 mL, 0.27 mmol) was added with an immediate color change from orange to green. The solution was stirred for 4 days with no further color change noted. As monitored by IR spectroscopy, upon addition of the phenylacetylene, the CO absorption changed from 1964 to 1943 cm^{-1}. The solution was concentrated to approximately 5 mL under reduced pressure, and pentane was added to yield a green precipitate. Upon filtration, the collected green solid was washed with pentane and dried in vacuo (0.080 g, 0.054 mmol, 80%).

(B) Method B. [(PCP)Ru(CO)(η^1-CH_2Cl_2)][BAr'_4] (**3**) (0.150 g, 0.10 mmol) was dissolved in 15 mL of CH_2Cl_2. Excess phenylacetylene was added, and the color of the solution changed to green. A new CO absorption was observed at 1943 cm^{-1} by IR spectroscopy. The volatiles were evaporated under reduced pressure. The resulting green residue was dissolved in 20 mL of tetrahydrofuran (THF) and heated to reflux for 3 h. After cooling to room temperature, the solution was concentrated to approximately 5 mL under reduced pressure, and 10 mL of pentane was added to yield a green precipitate. Upon filtration, the collected green solid was washed with pentane and dried in vacuo (0.130 g, 0.088 mmol, 86%). Crystals suitable for an X-ray diffraction study were obtained by slow diffusion of pentane into a CH_2Cl_2 solution of **8** at −20 °C. IR (CH_2Cl_2 solution): ν_{CO} = 1943 cm^{-1}. ^{1}H NMR (CD_2Cl_2, δ): 7.79 (1H, t, J_{HH} = 8 Hz), 7.73 (8H, br s, BAr'_4 phenyl), 7.57 (4H, br s, BAr'_4 phenyl), 7.34 (2H, d, J_{HH} = 8 Hz, phenyl), 7.10 (3H, overlapping multiplet, phenyl), 6.54 (2H, d, J_{HH} = 8 Hz, phenyl), 5.87 (1H, br s, PhC*H*), 3.40 (2H, m, PCP CH_2), 2.99 (2H, m, PCP CH_2), 1.43 (18H, vt, *N* = 15 Hz, PCP CH_3), 1.20 (18H, vt, *N* = 13 Hz, PCP CH_3). ^{13}C{^{1}H} NMR ($CDCl_3$, δ): 201.6 (t, J_{PC} = 12 Hz, *C*O), 162.0 (m, J_{BC} = 50 Hz, B−C_{ipso}), 155.2 (br s, Ru−*C*d=CHPh), 148.1−117.7 (multiple resonances due to aromatic carbons, olefin carbon, and *C*F_3), 39.6 (vt, *N* = 14 Hz, PCP *C*H_2), 37.3 (vt, *N* = 16 Hz, PCP *C*Me_3), 31.1, 28.8 (each a vt, *N* = 5 Hz, PCP *C*H_3). ^{31}P{^{1}H} NMR (CD_2Cl_2, δ): 37.4. ^{19}F NMR (CD_2Cl_2, δ): −63.2. Anal. Calc for $C_{65}H_{61}BF_{24}OP_2Ru$: C, 52.47; H, 4.13. Found: C, 52.42; H, 4.14.

NMR Study of Complex 3 with PhC≡CH in CD_2Cl_2. A screw cap NMR tube was charged with [(PCP)Ru(CO)(η^1-CH_2Cl_2)][BAr'_4] (**3**) (0.020 g, 0.014 mmol) in 0.6 mL of CD_2Cl_2. Phenylacetylene (∼5 μL, 0.04 mmol) was added, and an immediate color change from brown to green was observed. The reaction was monitored by ^{1}H and ^{31}P NMR spectroscopy. During the initial time, a single PCP−Ru species was observed with the following data. ^{1}H NMR (δ): 7.9−7.2 (overlapping aromatic rings), 6.54 (2H, d, J_{HH} = 8 Hz, phenyl), 6.55 (1H, t, *J* = 3 Hz), 3.90 (2H, m, PCP CH_2), 3.02 (4H, m, PCP CH_2), 1.62 (18H, vt, *N* = 15 Hz, PCP CH_3), 1.10 (18H, vt, *N* = 13 Hz, PCP CH_3). ^{31}P{^{1}H} NMR (δ): 31.5. The excess PhC≡CH was observed as a singlet at 3.15 ppm. During the reaction time, a new product appeared, as observed in ^{1}H and ^{31}P NMR spectroscopy. Features of the new product include a broad singlet at 5.87 ppm and two virtual triplets at 1.42 (*N* = 15 Hz) and 1.16 ppm (*N* = 13 Hz) in the ^{1}H NMR spectrum and a singlet at 37.4 ppm in the ^{31}P NMR spectrum. This is consistent with the formation of complex **8**. Over the reaction time, the decrease of the intensities due to the first product resonances was accompanied by an increase of the intensities of the resonances of complex **8**, and the resonance at 3.15 ppm due to the free PhC≡CH was not changed. After 4 days, complete conversion to complex **8** was achieved, as observed by both ^{1}H and ^{31}P NMR spectroscopy. Complex **8** was stable with excess PhC≡CH in CD_2Cl_2 for at least 48 h.

Computational Methods. Density functional and hybrid quantum mechanics/molecular mechanics (QM/MM) calculations were performed on truncated and full experimental models, respectively. The QM/MM approach was employed according to the ONIOM methodology.[83] For analysis of ligand (i.e., N_2, CH_2Cl_2, PhF) binding, the MM region contained three out of the four *tert*-butyl groups attached to the phosphorus atoms in each model; the *tert*-butyl group with an agostic interaction was chosen for QM modeling. The MM-modeled *tert*-butyl groups were described with the universal force field (UFF).[84] The QM region included the remainder of the molecule. Density functional theory (DFT),[85] using the B3LYP hybrid functional,[86−89] was employed for the QM core and in DFT calculations on truncated experimental models (*tert*-butyl groups were replaced by hydrogen; the phenyl substituent on the carbene and vinylidene ligands was replaced by hydrogen). Ruthenium and the main group elements were described with the Stevens (CEP-31G) relativistic effective core potentials (ECPs) and valence basis sets (VBSs).[90,91] The valence basis sets of the main group elements (carbon, nitrogen, oxygen, chlorine, and fluorine) were augmented as needed with a d polarization function with an exponent ($\xi_d = 0.80$), and a d polarization function with an exponent ($\xi_d = 0.55$) was used on phosphorus. For Ru complexes, the geometry was optimized for singlet cations, and all the geometries were fully optimized without any symmetry constraints. The Opt=NoMicro option was used to aid the convergence of ONIOM geometry optimizations. All calculations were performed using the Gaussian suite of programs.[92] When available, crystal structures for Ru complexes were used to initiate the geometry optimization calculations.

Acknowledgment. T.B.G. acknowledges the National Science Foundation (CAREER Award; CHE 0238167) and the Alfred P. Sloan Foundation (Research Fellowship) for support of this research and the research group of Professor Bruce Eaton for use of their argon-filled glovebox. T.R.C. wishes to acknowledge support by the Office of Basic Energy Sciences, United States Department of Energy, through Grant DOE-FG02-97ER14811. Calculations employed the UNT computational chemistry resource, for which K.A.B. and T.R.C. acknowledge the NSF for support through Grant CHE-0342824.

Supporting Information Available: Files (cif) for structures of complexes **2**, **3**, **4**, **7**, and **8** and all structures calculated by DFT, optimized structures for computed ruthenium complexes, and discussion of the X-ray structure of complex **4**. This material is available free of charge via the Internet at http://pubs.acs.org.

IC051074K

(83) Vreven, T.; Morokuma, K. *J. Comput. Chem.* **2000**, *21*, 1419−1432.
(84) Rappé, A. K.; Casewit, C. J.; Colwell, K. S.; Goddard, W. A., III; Skiff, W. M. *J. Am. Chem. Soc.* **1992**, *114*, 10024−35.
(85) Parr, R. G.; Yang, W. *Density-functional Theory of Atoms and Molecules*; Oxford University Press: Oxford, 1989.
(86) Becke, A. D. *Phys. Rev.* **1998**, *A38*, 3098−3100.
(87) Becke, A. D. *J. Chem. Phys.* **1993**, *98*, 1372−1377.
(88) Becke, A. D. *J. Chem. Phys.* **1993**, *98*, 5648−5652.
(89) Lee, C.; Yang, W.; Parr, R. G. *Phys. Rev.* **1998**, *B37*, 785−789.
(90) Stevens, W. J.; Basch, H.; Krauss, M. *J. Chem. Phys.* **1984**, *81*, 6026−6033.
(91) Stevens, W. J.; Krauss, M.; Basch, H.; Jasien, P. G. *Can. J. Chem.* **1992**, *70*, 612−630.
(92) Frisch, M. J.; Trucks, G. W.; Schlegel, H. B.; Scuseria, G. E.; Robb, M. A.; Cheeseman, J. R.; Zakrzewski, V. G.; Montgomery, J. A., Jr.; Stratmann, R. E.; Burant, J. C.; Dapprich, S.; Millam, J. M.; Daniels, A. D.; Kudin, K. N.; Strain, M. C.; Farkas, O.; Tomasi, J.; Barone, V.; Cossi, M.; Cammi, R.; Mennucci, B.; Pomelli, C.; Adamo, C.; Clifford, S.; Ochterski, J.; Petersson, G. A.; Ayala, P. Y.; Cui, Q.; Morokuma, K.; Rega, N.; Salvador, P.; Dannenberg, J. J.; Malick, D. K.; Rabuck, A. D.; Ragavachari, K.; Foresman, J. B.; Cioslowski, J.; Ortiz, J. V.; Baboul, A. G.; Stefanov, B. B.; Liu, G.; Liashenko, A.; Piskorz, P.; Komaromi, I.; Gomperts, R.; Martin, R. L.; Fox, D. J.; Keith, T.; Al-Laham, M. A.; Peng, C. Y.; Nanayakkara, A.; Challacombe, M.; Gill, P. M. W.; Johnson, B.; Chen, W.; Wong, M. W.; Andres, J. L.; Gonzalez, C.; Head-Gordon, M.; Replogle, E. S.; Pople, J. A. *Gaussian 98*, revision A.11.3; Gaussian, Inc.: Pittsburgh, PA, 2002.